CHAPTER 6 - REACTION OF THE INTRUSIVE ROCKS WITH THE COUNTRY ROCKS AND WITH XENOLITHS

6.1 Previous work on xenoliths

In the Uitkomst Complex the dominant xenolith type is a calc-silicate rock of variable composition derived from the Malmani Subgroup (Gomwe, 2002; van Zyl, 1996; Gauert, 1996; de Waal et al. (2001), Maier et al., 2004). The contact aureole of the Uitkomst Complex extends 50 to 100 m from the contact into the country rock. Within the aureole, the Malmani Dolomite has been transformed to calc-silicate hornfels grading to talc-tremolite-bearing carbonate rock (Gauert et al., 1996; Gomwe, 2002). The calc-silicate xenoliths are composed mainly of diopside, epidote, calcite and tremolite (Gomwe, 2002). As indicated before, the calc-silicate rocks seem to have suffered very little or no rotation, with the preserved internal layering being sub-parallel to the igneous layering (Gomwe, 2002). The pelitic roof material of the complex underwent medium- to high-grade metamorphism extending 10 to 50 meters above the Complex, represented by a rim of corundum-andalusite-hornfels (Gauert et al., 1996; Hornsey, 1999; Gomwe, 2002). The interaction between the xenoliths and the LHZBG magma and inferred influence on mineralization within this unit was the subject of a dissertation by Hulley (2005).

Considering other intrusions of a similar nature, the Platreef is the most relevant. Gain and Mostert (1982) found that the main mineral assemblages of the xenoliths in the Platreef consist of variable amounts of fosterite, diopside and monticellite. Retrograde metamorphism of these xenoliths led to the alteration of the original minerals assemblage in the following manner: fosterite alters to serpentine, monticellite alters to hydrogrossular, talc and serpentine and diopside alter to hydrogrossular, talc and tremolite. Brucite was found to be the most common alteration product of dolomite xenoliths (Gain and Mostert, 1982). The contacts between the xenoliths and the Platreef rocks are rarely sharp, but pegmatoidal (Gain and Mostert, 1982).

6.2 Xenoliths investigated during the current investigation

There are two types of calc-silicate xenoliths present in the core samples investigated from the Uitkomst Complex. The first type is "clean" xenoliths (Figure 6.6) with a white appearance, usually displaying a sharp contact relationship with the host pyroxenite. White xenoliths usually appear “cleaner” due to the expulsion of contaminants such as carbon during thermal metamorphism (Park and MacDiarmid, 1975). A petrological investigation of these xenoliths reveals that they consist mainly of clinopyroxene and calcite (Figure 6.1). Zones of larger clinopyroxenes (diopside) that show signs of uralitization occur near the contact between the xenolith and the pyroxenite, while smaller subhedral crystals of clinopyroxene and calcite showing no signs of alteration (Figure 6.2 and 6.3) are in close contact with these larger clinopyroxene grains, and occur towards the centre of the xenolith. It has been determined by Tilley and Harwood (1931) that by the addition of CO_2 during breakdown of carbonate rocks assists in decreasing the viscosity of the melt and this allows free growth of comparatively large crystals. Similar decarbonation reactions are probably responsible for the development of the larger diopside crystals near the xenolith-pyroxite contact, relative to the interior of the xenolith. Minor amounts (<10 %) of blebby pyrite are present in these xenoliths (Figure 6.2). These pyrite grains generally occur along the preserved bedding of the dolomite protolith (Figure 6.9). The pyrite grains are interstitial to the clinopyroxene grains and show no alteration features.

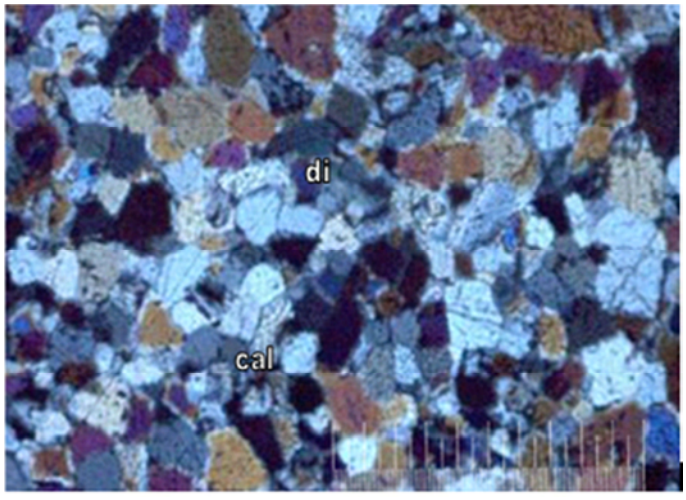

Figure 6.1. The“clean xenolith” consist mainly of small diopside (di) (high birefringence minerals) and calcite (cal) (blue-grey low birefringence minerals) grains. The picture scale bar is 1000 micron and the image was taken with cross-polarized light. (Sample CS21).

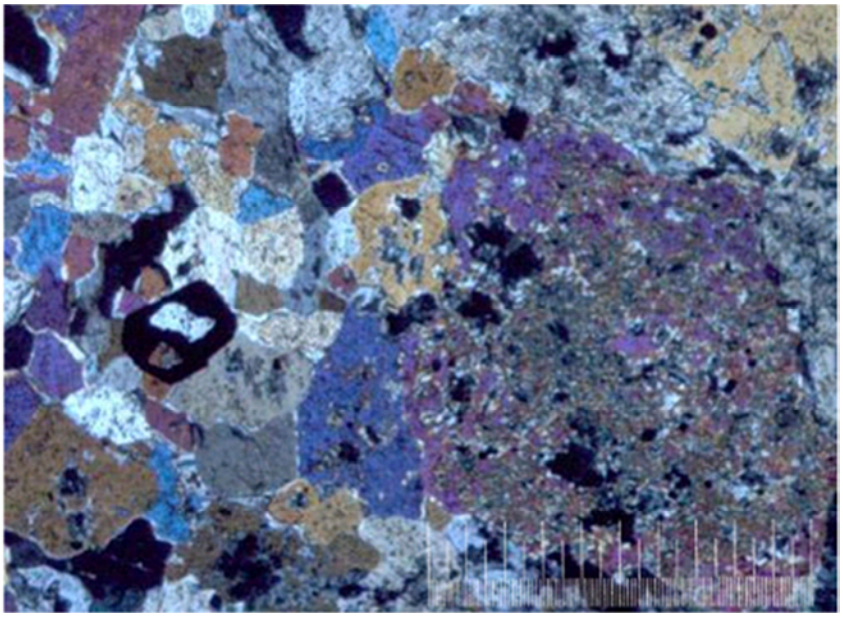

Figure. 6.2. Photomicrograph showing large clinopyroxene (high birefringence) grains that has been uralitized (right side of picture) in contact with smaller, unaltered clinopyroxene grains (left side of picture). There is no compositional difference between the two textures. Also present are carbonate minerals (low birefringence) and sulphide (pyrite) grains (black). The picture scale bar is 1000 micron and the image was taken with cross-polarised light. (Sample UK44G).

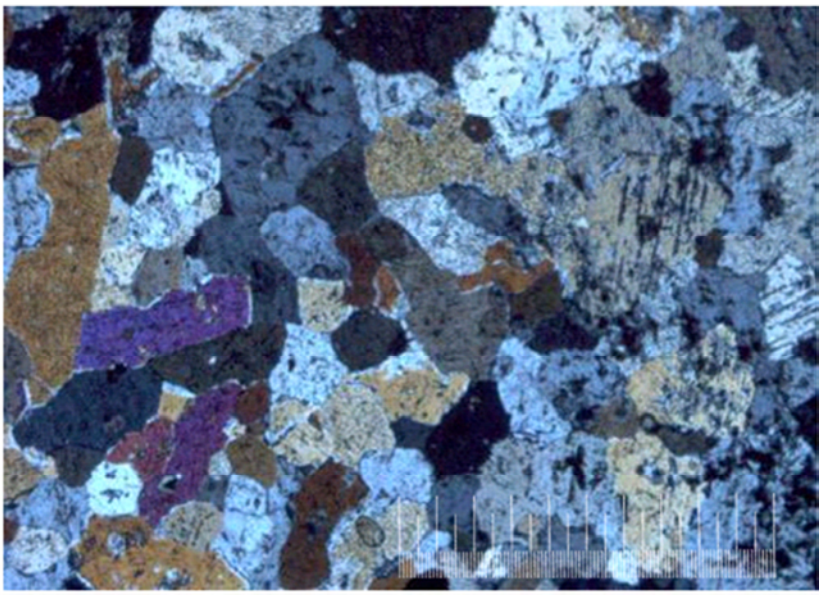

Figure. 6.3. Photomicrograph showing slightly uralitized clinopyroxene (high birefringence) and carbonate (low birefringence) grains. The picture scale bar is 1000 micron and the image was taken with cross-polarized light. (Sample CS21).

The second variety of xenoliths is described as "contaminated" xenoliths. These xenoliths have a grey colour and contain apophyses of pyroxenite running through them (Figure 6.7). The xenoliths have slightly larger amounts (> 10%) of pyrite present. They consist largely of altered pyroxene, amphiboles and muscovite and phlogopite (Fig.6.4 and 6.5).

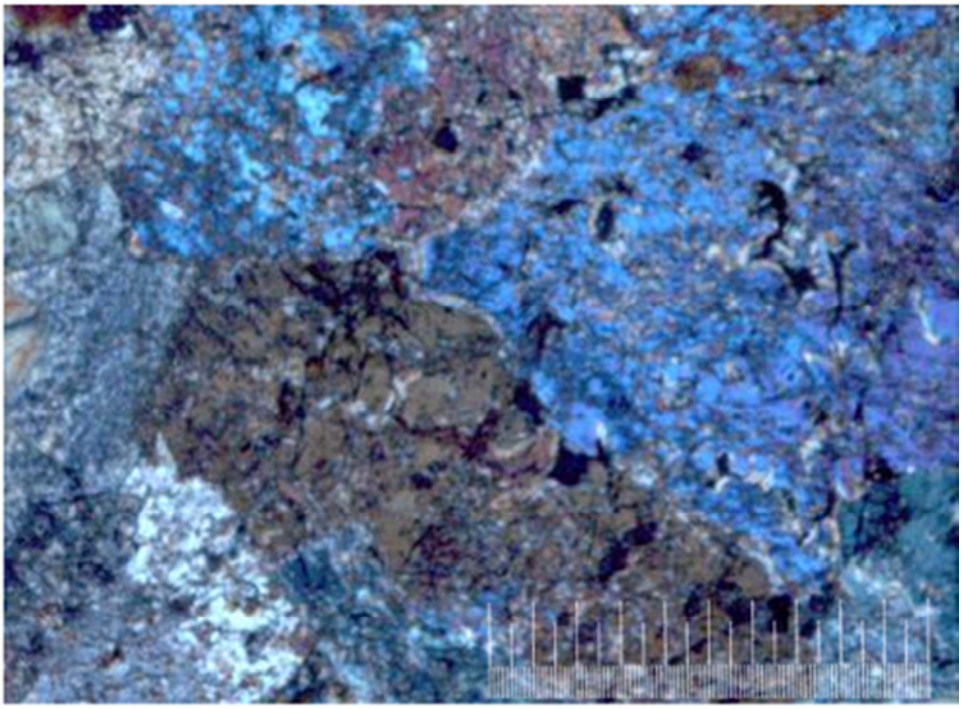

Figure 6.4 Large grains of uralized clinopyroxene in a “contaminated” xenolith. The picture scale bar is 1000 micron and the image was taken with cross-polarized light. (Sample UK3N).

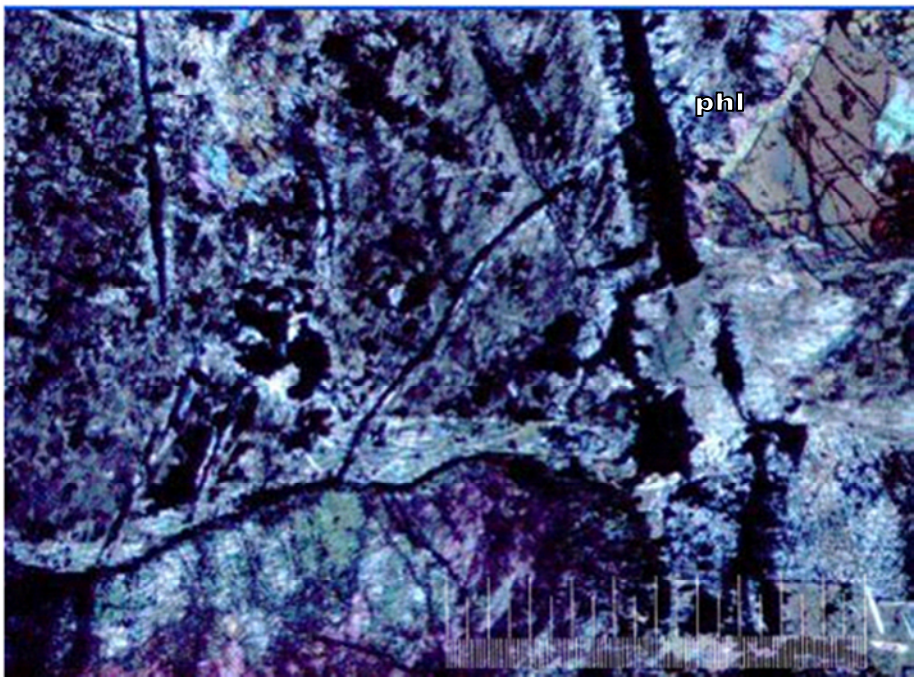

Figure 6.5. A highly altered "contaminated" xenolith. Pseudomorphous serpentine (fiberous white), magnetite (black stingers) after olivine and amphibole, chlorite (high to intermediate birefringence) after pyroxene respectively. Some phlogopite (phl) (brown mineral, top right) are also present in this section. The picture scale bar is 1000 micron and the image was taken with cross-polarised light. (Sample CS4).

The xenoliths display a variety of textural relationships at their contacts with the magmatic material. The first relationship is formed by a very fine-grained zone, dark in colour and consisting of highly altered minerals (Figure 6.6). This is associated with the "clean" xenoliths. A zone of what appears to be primary phase minerals forms the second type of contact relationship, consisting mainly of pyroxene grains inside the xenolith which are, altered to actinolite (Figure 6.7). Some muscovite, phlogopite, pyrite and pyrrhotite are also present. The third contact relationship comprises pegmatoidal material, consisting of coarse large pyroxene (diopside) grains and calcite, with interstitial coarse grains of sulphide minerals (Figure 6.8). The massive sulphide bordering the pegmatoidal material consists mainly of pyrrhotite with minor chalcopyrite and pentlandite with small Platinum Group Mineral (PGM) grains. This is in direct contrast to the sulphides inside the xenolith that consist of pyrite only. There appears to be no difference in the development or abundance

of pegmatoidal material at the bottom or top of the xenoliths, as determined during the current and previous investigations (Steenkamp, 2004).

Figure 6.6. Sharp contact between a clean xenolith and pyroxenite from the LHZBG in a quartered core sample. The contact is fine grained, dark and consists of a highly altered material. Where a "clean" xenolith can be seen on the right and pegmatiodal pyroxenite to the left. (Sample CS21).

Figure 6.7. A vein of pyroxenite penetrating a xenolith. On the contact a layer of uralized pyroxenes are developed. Disseminated sulphides may also be seen close to the contact. (Sample CS21).

Figure 6.8 An example of a pegmatiodal contact. The xenolith was situated to the left side (not sampled) of the sample. Large uralized clinopyroxene grains occur on the contact and extend away from the contact. Massive sulphides surround them. A large white calcite grain is also present. The pegmatoidal material grades into wehrlite on the far right hand side of the sample. (Sample CS13).

Figure 6.9. Blebby pyrite mineralization in a xenolith. The pyrite mineralization occurs along the preserved original bedding of the dolomite protolith. (Samples UK3R top and UK3S bottom).

6.3 Melting rate of xenoliths

It is important to consider the melting rate of xenoliths in magma to explain some of the inferred textural observations in the Uitkomst Complex. The melting of crustal xenoliths is rapid compared to other magmatic processes. The rate is however controlled by the magmatic temperature, initial xenolith temperature, melting temperature and melt viscosity and the composition of the xenolith. This provides an efficient mechanism for producing

changes in the compositional as well as thermal properties of the intruding magma. Cooling of magma in the thermal boundary layer adjacent to the xenolith is relatively restricted, thus any induced crystallization will be limited and unlikely to have an appreciable direct influence on the dynamics of the magma's thermal convection around the xenolith. The thickness of the mobile mush layer around the xenolith is predicted to be typically only a few centimetres. The melting rate of continental crust xenoliths has been determined McLeod, Stephen and Spark, (1998) to be about 2mm/hr, based on experiments done involving stationary and sinking wax balls in hot liquid.

Partial melting of non-eutectic compositions may produce a layer of crystal melt mush at the contact with the xenolith. Such processes may have given rise to the pegmatoidal material surrounding some of the xenoliths in the LHZBG Unit.

It should however be noted at this point that most work pertaining to skarn formation have been based on the interaction between felsic (granitic) intrusion and dolomitic country rocks. Dolomite only melts at very high temperatures, but undergoes a series of decarbonation reactions at lower temperatures (Bowen, 1940). Care should be taken to distinguish the difference in interaction and in product between a volatile-rich felsic- and volatile-poor mafic magma. The effects of assimilation and the collapse of dolomitic xenoliths in a mafic magmatic environment is described in locations such as Ioko-Dovyren intrusion in Russia (Wenzel et al., 2004 and Wenzel et al., 2005) and at the Panzhihua deposit in China (Ganino et al. 2008).

It was determined by Glazner (2007) that the assimilation of wall rock by an intruding mafic magma would be limited due to the energy required. Glazner suggest that the process of disaggregation without melting will result in greater assimilation, without requiring as much energy. The experimental data (Glazner, 2007) suggest that during disaggregation, the assimilation of cool xenoliths requires significant crystallization of the host magma. Larger crystallization is observed during disaggregation, relative to a fully reacted case. This is suggested (Glazner, 2007) to be as a result of partial crystallization of the host magma in

order to heat the xenolith, without xenolithic crystals being resorbed. The amount of crystallization by the host magma becomes important because it influences the ability of the host magma to incorporate the xenolith material and its own ability to rise. Crystallization above 50% also significantly changes the viscosity of the magma by several orders of magnitude, making the magma semi-rigid. At this level of crystallization any segregation of magmatic liquid would be very limited. It is also suggested by Glazner (2007) that addition of new magma is required to counter the effect of heat loss that will otherwise create an upper boundary for the assimilation of xenoliths.

A semi-quantitative estimation may be made based on the information contained in the borehole logs of to the period during which the magma was exposed to the effect of assimilation of dolomite. This is done by measuring the vertical thickness of the host rock between the preserved xenolith inclusions in the LHZBG Unit. The thickness of these intervals is then related to the calculated assimilation time and a period of static exposure is calculated. Assumptions for these calculations are:

1) That dolomites were present up to the level represented by the current top contact of the LHZBG Unit.

2) That all of the dolomite country rock was either assimilated or removed from the system.

3) Accepting that thin pyroxenite layers within xenoliths were not included as separate layers in the logs.

4) Static system is assumed, whereas in reality the magma was probably flowing through a conduit.

The calculated values are given in Table 6.1. As could be expected the top of the LHZBG Unit was exposed to the longest period of interaction and assimilation of dolomite by the intruding magma. The calculated periods for the succession lower in the unit are highly variable with height and spatial distribution.

Table 6.1. The thickness of the area between xenoliths is indicated under the borehole number from the top to the base of the LHZBG Unit and the hours (calculated for 2mm/hour) indicated in bold.

UK3	Hours	UK12	Hours	UK20	Hours	UK32	Hours	UK39	Hours
1.8	**90**	6.64	**332**	19.41	**970.5**	7.79	**389.5**	25.06	**1253**
3.59	**179.5**	0.43	**21.5**	1.36	**68**	0.36	**18**	1.12	**56**
0.55	**27.5**	1.44	**72**	3.43	**171.5**	3.12	**156**	3.97	**198.5**
2.44	**122**	0.72	**36**	0.76	**38**	0.26	**13**	1.49	**74.5**
3.05	**152.5**	2.66	**133**	3.92	**196**	0.41	**20.5**	4.55	**227.5**
4.08	**204**					0.91	**45.5**	0.21	**10.5**
1.38	**69**					1.31	**65.5**	2.01	**100.5**
1.23	**61.5**					0.2	**10**	0.66	**33**
0.64	**32**					23.73	**1186.5**		
2.04	**102**					6.38	**319**		
2.84	**142**								
1.52	**76**								
0.97	**48.5**								

Table 6.1. Cont.

UK40	Hours	UK43	Hours	UK44	Hours	UK55	Hours	UK57	Hours
13.65	**682.5**	6.97	**348.5**	7.02	**351**	6.09	**304.5**	0.57	**28.5**
0.29	**14.5**	0.17	**8.5**	1.15	**57.5**	6.08	**304**	1.31	**65.5**
4.32	**216**	30.41	**1520.5**	0.66	**33**	0.23	**11.5**	2.62	**131**
0.16	**8**	0.28	**14**	0.7	**35**	0.6	**30**	0.2	**10**
0.17	**8.5**	3.43	**171.5**	0.52	**26**	4.34	**217**	2.26	**113**
6.61	**330.5**	0.44	**22**	0.54	**27**	3.2	**160**	0.53	**26.5**
0.99	**49.5**	7.95	**397.5**	0.19	**9.5**	0.17	**8.5**	1.23	**61.5**
		0.17	**8.5**	0.79	**39.5**	2.09	**104.5**	0.55	**27.5**
		3.88	**194**	0.22	**11**	9.36	**468**	6.77	**338.5**
				5.32	**266**			1.11	**55.5**
				0.26	**13**			1.86	**93**
				0.28	**14**			0.33	**16.5**
				4.82	**241**			0.97	**48.5**
				2.93	**146.5**			2.43	**121.5**
				2.88	**144**			5.29	**264.5**

Table 6.1. Cont.

UK60	Hours	UK61	Hours	UK 63	Hours	UK 65	Hours	UK68	Hours
17.73	**886.5**	9.31	**465.5**	24.03	**1201.5**	2.27	**113.5**	8.44	**422**
2.94	**147**	2.99	**149.5**	7.86	**393**	11.48	**574**	0.06	**3**
0.45	**22.5**	4	**200**	2.19	**109.5**			15.27	**763.5**
1.65	**82.5**	0.54	**27**						
2.78	**139**	28.64	**1432**						
2.94	**147**								
0.61	**30.5**								
0.44	**22**								
6.44	**322**								
1.34	**67**								

6.4. Distribution of Xenoliths and their Effect on the Development of the Uitkomst Complex

The distribution of boreholes is indicated by Figure 6.10. The true thickness of the LHZBG Unit and the percentage of xenoliths in the LHZBG Unit for certain sections were calculated. The true thickness of the BGAB was also calculated. The results are presented in figure 6.11 to figure 6.13.

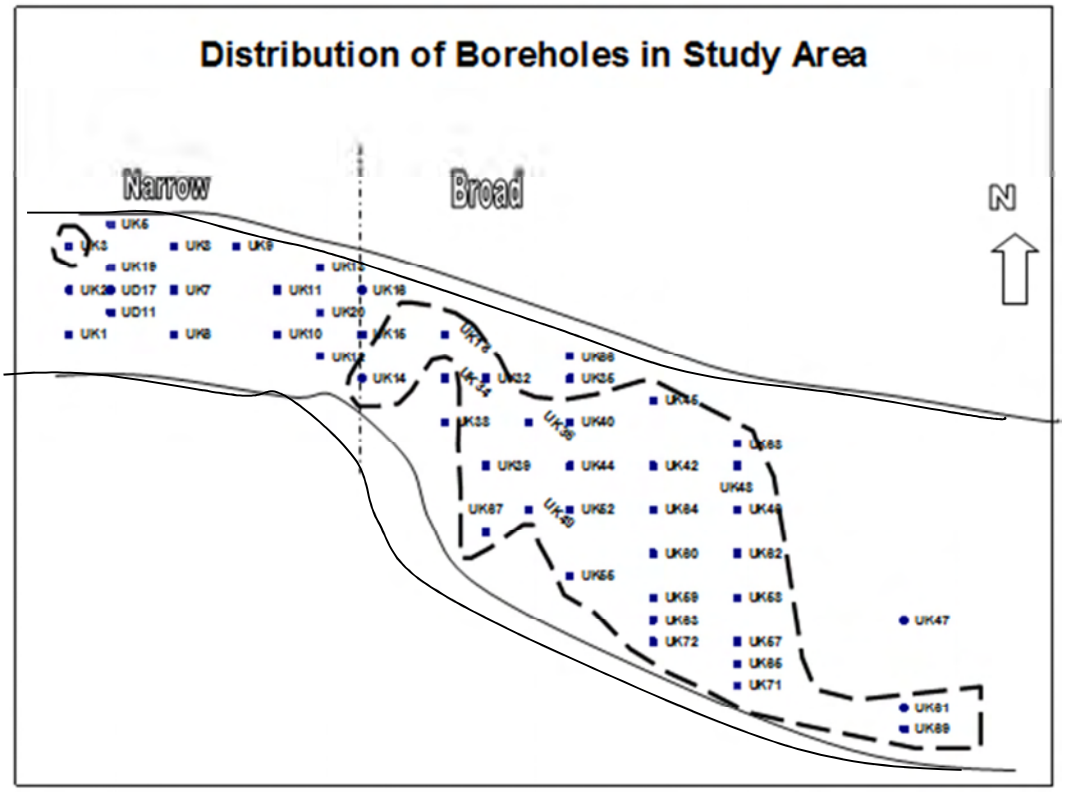

Figure 6.10. The position of boreholes in the study area. The "talc-rich" zone is indicated by the dashed line (After L. Bradford, 1996). The inferred margins of the Uitkomst Complex are indicated by the solid black lines. To the left of the stripe-dash line is the narrow part of the intrusion and to the right the broad part. The base of the picture represents approximately 2 kilometers.

First the percentage of xenoliths in the LHZBG Unit in the study area is compared to the thickness of the LHZBG and BGAB Units in the study area by looking at selected sections (north-south) through the Complex. These calculations are based on the borehole logs prepared by the AVMIN geologists during the feasibility programme during the 1990s. Secondly, these will be evaluated in terms of the distribution of the "talc-rich" zone located in the study area.

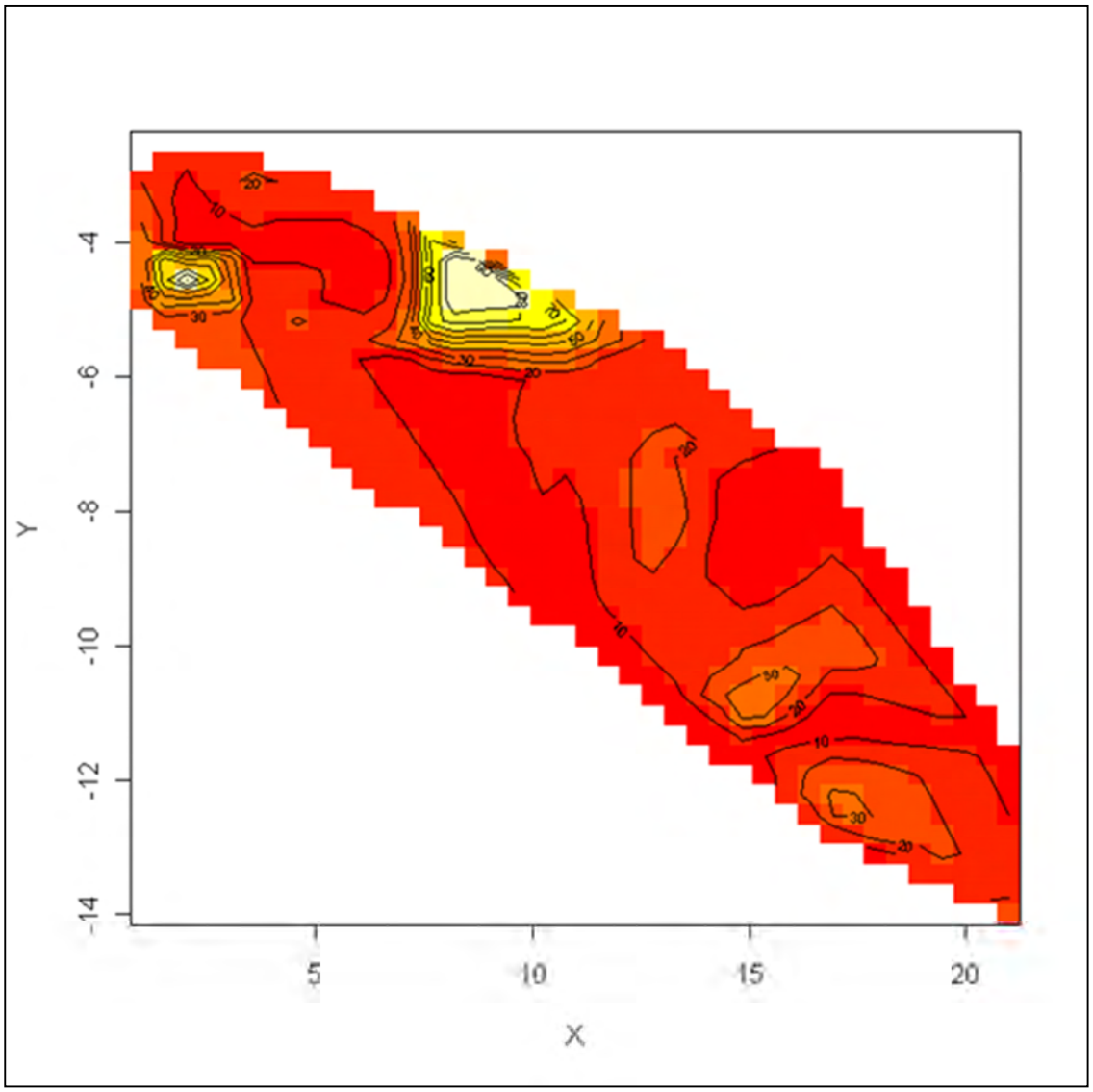

Figure 6.11. Contour map indicating the percentage distribution xenoliths in the study area of the Complex. The graph was constructed using an interpolation routine included as part of the "AKIMA" package for the functional language "R" and based on Akima (1978). A false X- and Y-coordinate system is applied.

The percentage of xenoliths (figure 6.11), the true thickness of the LHZBG Unit (figure 6.12) and of the BGAB Unit (figure 6.13) is considered in this discussion. The true thickness refers to the thickness of the unit after the thickness of post-Uitkomst diabase intrusions has been subtracted. The figures were constructed utilizing the "AKIMA"

package and show contour intervals of ten. A false X- and Y-coordinate system was used to construct the graphs.

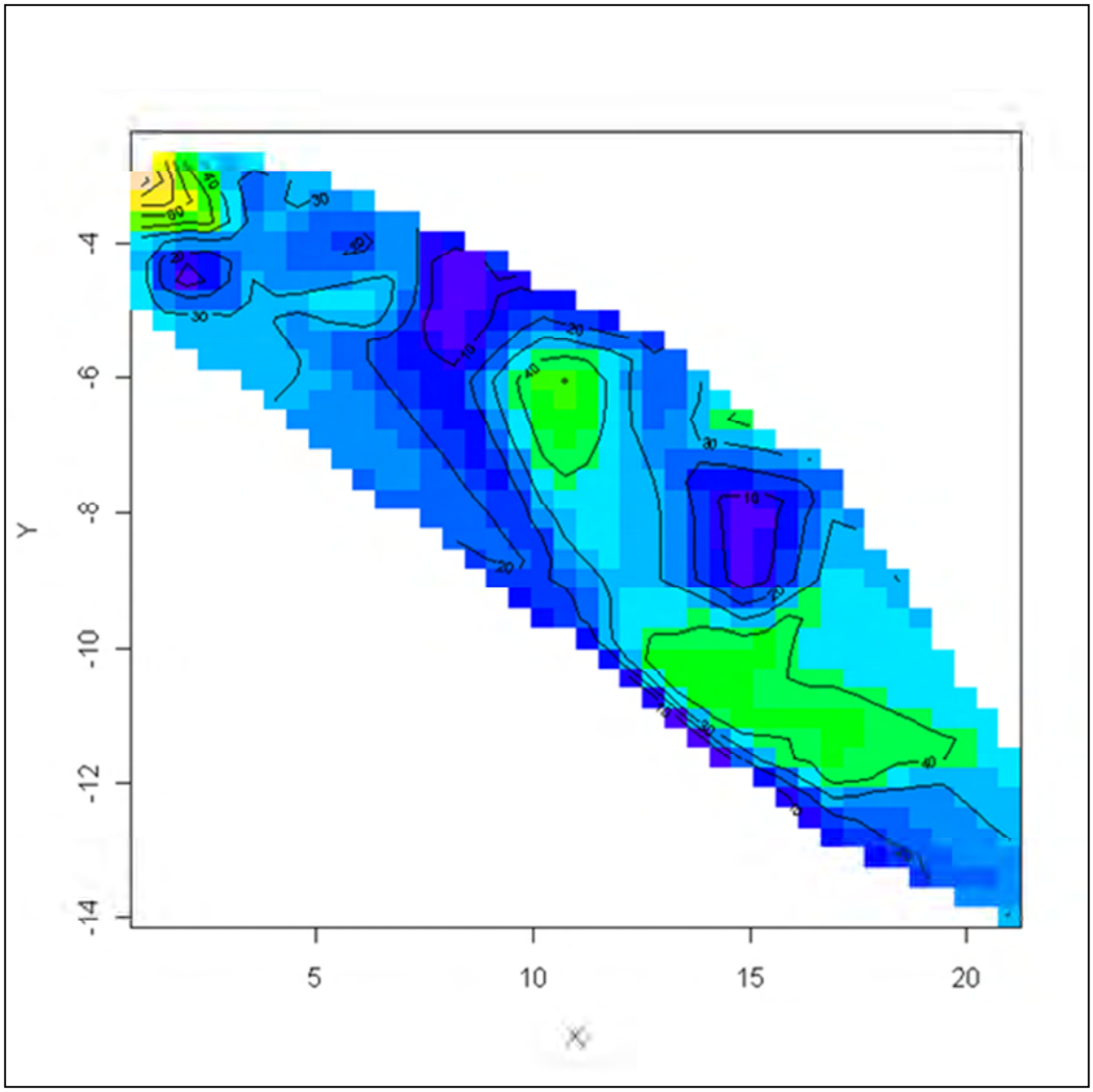

Figure 6.12. Contour map indicating the true thickness distribution of the LHZBG Unit in the study area of the Complex. The graph was constructed using an interpolation routine included as part of the "AKIMA" package for the functional language "R" and based on Akima (1978). A false X- and Y-coordinate system is applied.

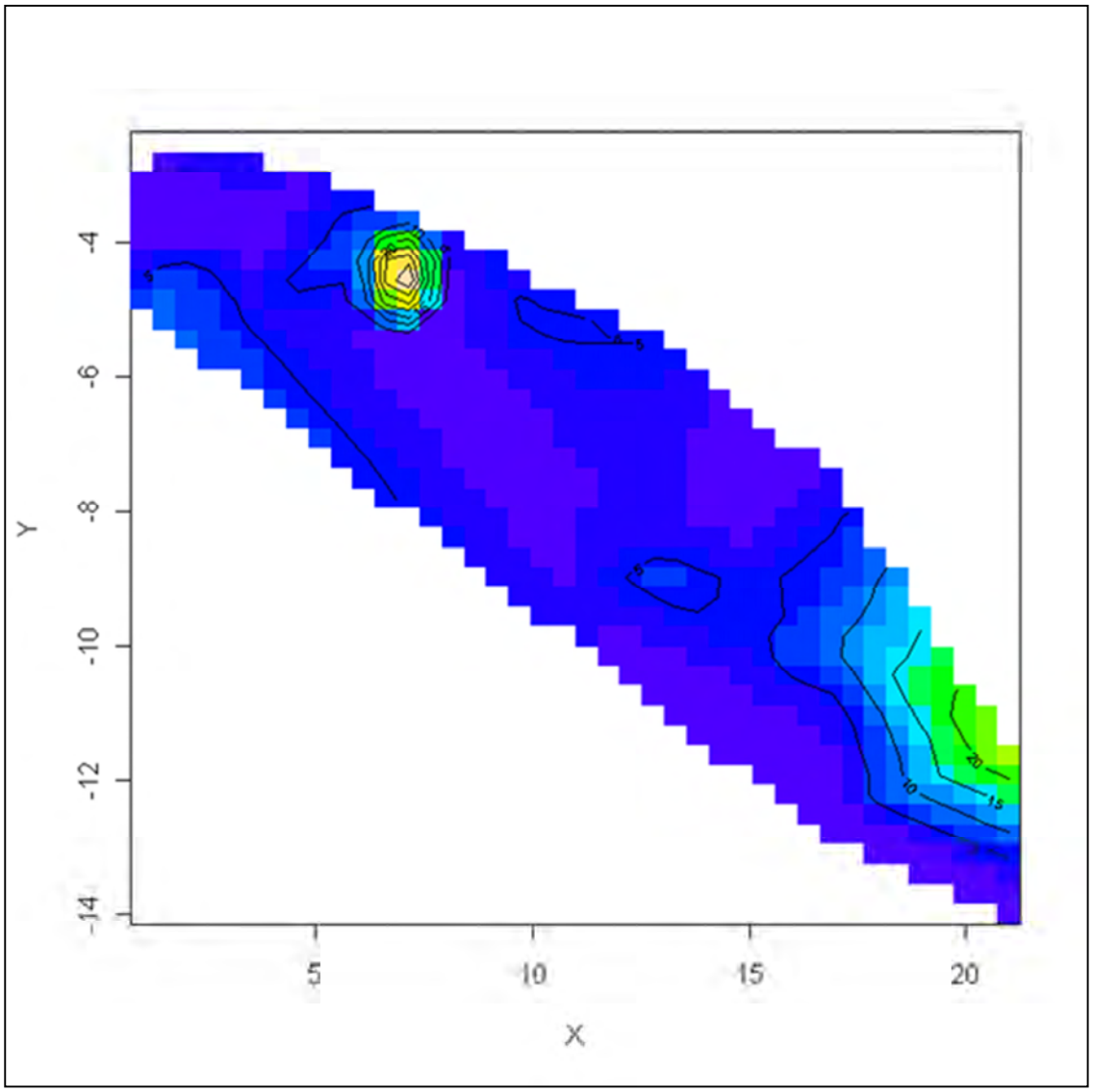

Figure 6.13. Contour map indicating the true thickness distribution of the BGAB Unit in the study area of the Complex. The graph was constructed using an interpolation routine included as part of the "AKIMA" package for the functional language "R" and based on Akima (1978). A false X- and Y-coordinate system is applied.

In the narrower part of the intrusion, in the upper northwest of the study area, there appears to be a weakly defined relationship between the percentage of xenoliths in the LHZBG Unit and the thickness of the LHZBG Unit. Where the LHZBG Unit is the thickest, the percentage xenoliths are lower than where the LHZBG Unit is the thinnest. It also appears as if the intrusion “meandered”, from the northeast of the complex, first toward the north

and then to the south and then to the center, relative to the inferred margins of the Complex. There also appear to be a weak correlation between the distribution and thickness of the BGAB Unit and the distribution of the xenoliths. Where the BGAB Unit is thickest, the percentage of xenoliths also appears to attain its maximum occurrence in the LHZBG Unit. There is also a very weak correlation between the distribution and thickness of the BGAB Unit and the overlying LHZBG Unit. Where the BGAB Unit is thickest, the LHZBG Unit appear thinnest and where the BGAB Unit is thinnest, the LHZBG Unit appears thickest. The BGAB Unit appear to be thickest in the southern part of the study area.

In the broader part of the intrusion in the study area, the weakly defined relationship between the percentage of xenoliths present in the LHZBG Unit and the thickness of the LHZBG Unit defined above cannot be discerned. However, it appears as if the intrusion also "meandered" in the broad part of the intrusion. From the northwest of the Complex, the intrusion appear to have first "meandered" to the south, then to the north, back to the south and finally more consistently to the north in the southeast of the Complex. In the broader part of the Complex the percentage xenoliths attains its maximum percentage towards the northern inferred margin of the Complex in the northwest. Where the xenoliths constitute 100%, it is inferred to represent a part of the Complex that only has finger-structures into the surrounding country rock. Towards the south-west part, of the broader part of the Complex, the xenoliths appear to maintain its maximum percentage to the south of the idealized center of the Complex, relative to the inferred margins of the Complex.

As in the narrow part of the Complex there appear to be a weak correlation between the distribution of the BGAB Unit and the distribution of xenoliths in the broader part of the Complex. Where the BGAB Unit is thickest, the percentage xenolith in the LHZBG Unit attains it highest occurrence. This correlation is however completely reversed in the south east part of the study area. In the south east of the broader part of the Complex, the percentage xenoliths now attain its maximum where the BGAB Unit is thinnest. There also appear to be a weak correlation between the distribution and thickness of the BGAB and the LHZBG Units. In the broader area the BGAB Unit is thickest, the LHZBG Unit is also

thickest. The BGAB Unit have been preserved in the southern and south-central parts of the intrusion in the broader part of the Complex.

There is no apparent correlation between the location of the "talc-rich" zone in the study area relative to the percentage of xenoliths in the LHZBG Unit, nor to the distribution of the LHZBG Unit in the study area. Nor is there any correlation between the thickness or distribution of the BGAB Unit and the "talc-rich" zone in the study area. It may be noted that the "talc-rich" zone is located in the area where the LHZBG Unit of the intrusion is thickest in the central part of the Complex. It is also considered significant that the "talc-rich" area is located in the broadest part of the intrusion in the study area. The effect of the broadening of the Complex, and the distribution of the MCR layer will be considered in a later section.

The formation of the skarn aureole may also have been instrumental in the formation of an economically viable LHZBG Unit. At the Noril'sk intrusion, Arndt et al. (2005) suggested that the magma parental to the ore deposit is related to the physical factors which influenced interaction with the wall rock. The first is a magma with a high metal tenor and low volatile content which was able to interact with the wall rocks. The second is that the magma bypassed the magma chamber, not interacting with the granitic crust, which would have resulted in sulphide segregation at an inaccessible depth. This magma was then left relatively uncontaminated and able to assimilate evaporates and segregate sulphides at a shallow (mineable) level.

The Uitkomst Complex is intruded between the Archean basement granite and the overlying sedimentary sequence of the Transvaal basin. Intrusion of the LHZBG magma and the resultant formation of a skarn aureole below it, would have shielded the main intruding LHZBG magma from direct interaction with the Archean granite. Had the LHZBG magma intruded directly on the Archean granite, it is possible that the magma would have segregated sulphides at depth. The magma however was now able to intrude to much shallower levels. Here the magma partially assimilated dolomite country rock, which led to

an increase of oxygen fugacity and addition of sulphur, which resulted in the segregation of the sulphides at shallow (mineable) depth. The skarn floor would also have increased turbulent magma flow in the conduit and the opportunity for segregated sulphide droplets to accumulate. It is suggested in section 2.1.3 that where the LHZBG is in contact with the floor rocks, it is due to scouring of the BGAB.

It was noted that blebby pyrite occur along the preserved bedding of the xenoliths. The formation of this feature may be due to the intrusion of the LHZBG magma which mobilized a fluid in the dolomitic precursor rock, resulting in pyritization taking place along the preserved bedding in the xenoliths. This phenomenon may also be used as prove that the skarnification event took place synchronous to the intrusion of the LHZBG magma.

6.5 Petrogenetic implication for the Uitkomst Complex

In the Uikomst Complex the xenoliths consist dominantly of diopside. The diopside composition suggests thermal metamorphism of siliceous dolomite. The xenoliths also contain minor amounts of calcite, actinolite and chlorite. The presence of these alteration minerals suggests the presence of hydrous fluids, either inside the xenoliths during skarn mineralization or a late stage fluid infiltrating the xenolith as suggested by Hulley (2005). The increase in grain size of the diopside closer to the edge of the xenoliths may indicate annealing of the grains due to the presence of a CO_2-rich fluid. Such a fluid could have concentrated near the contact of the xenolith and the intruding magma. The CO_2-rich fluid initially lowers the viscosity favouring the growth of the diopside, but it also leads to the subsequent uralization of the grains. The variability of the CO_2 content during the skarn mineralization is demonstrated by the variation of in mineralogy of the xenoliths. In xenoliths from borehole SH176 (studied during the author's reconnaissance investigation on Slaaihoek) the presence of grossular and complete lack of sulphide mineralization would suggest lower CO_2 concentration at the time of formation relative to xenoliths from the current study area.

The role of temperature and CO_2 pressure in the formation of skarns, and its bearing on mineralization was investigated by Shoji (1975). This study determined that the most favourable skarn-forming conditions exist below 400 ˚C and at a CO_2 pressure with upper and lower limits determined by the stability of grandite garnet and the instability of hydrogrossular respectively. The amount of CO_2 in the fluids was thus inferred to be between 0.7 and 2.0 mole percent at 400 ˚C. These values need to be revised for the formation of iron-rich clinopyroxene. It was also pointed out that CO_2 needs to be released efficiently for skarn mineralization to proceed. Shoji (1975) stressed the importance of the availability of iron in the ore-forming fluid, as the ore-minerals are found in association with pyroxene and garnet skarns.

It appears from borehole logs that more xenoliths may have been preserved in the broader part of the intrusion away from the edge of the Uitkomst Complex, with the exception of finger-structures protruding from the Complex into the country rock, in the narrow part of the Complex. The preservation of horizontal bedding would suggest a more passive style of intrusion.

The presence of pyrite mineralization along the original bedding of the dolomite precursor rock and chlorite in the xenoliths may indicate a later intrusion of the xenoliths by a sulphur-rich hydrothermal fluid with a temperature of up to 400 ˚C and low to intermediate CO_2 content (Hulley, 2006). An alternative to this model is discussed below.

The concentration of iron sulphides in sediments is usually sparsely disseminated crystal and crystalline aggregates of pyrite or marcasite (Stanton, 1972). Enrichment may be due to pyritization of sedimentary iron oxide concentrations which already deposited during sedimentation (Stanton, 1972). This may be due to “leaking” of H_2S from underlying sediments. Alternatively, the iron accumulated during sedimentation will aid in the precipition of sulphide from pore water. It is known that magmatic material contains heavy metal halides (mainly chlorides), which will dissolve in pore water. The pore water will be driven away form the intrusion and dispersed. As this pore water, laden with iron and other elements like copper lead and zinc, is dispersed it may encounter the disseminated iron

sulphides. These metals will displace some of the iron from the existent iron sulphides and precipitate as sulphides themselves. This metamorphic concentration is expected to cease once the rock ceases to contain free water (Stanton, 1972). The formation of pyrite cubes in this type of low-grade metamorphic environment is not well understood, but it is suggested that these grains form due to "retexturing" of concretions or by coalescence of closely packed groups of smaller crystals (Stanton, 1972).

In the alternative model suggested here, the pyrite occurring along the preserved bedding of the xenolith formed during emplacement of the LHZBG magma and the resultant skarnification process which affected the dolomitic precursor rock. The implication is that the LHZBG intruded at a level above the current preserved xenolith horizon, stoping downward into the country rock. The intruding LHZBG magma may have contained Fe-rich halides, which would then dissolve in the pore water present in the dolomite country rock. The pore water would be driven away from the intruding magma, into the surrounding country rock. As the pore water, now laden with Fe-rich halide complexes, was dispersed through the underlying country rock it encountered pyrite or marcasite, likely deposited during diagenesis of the dolomite along the original bedding planes. The pore water would interact with these pyrite or marcatite grains, displacing some of the iron in the sulphides and precipitating as sulphides themselves. This process may have been active while free water was still able to circulate in the forming xenoliths. The mineralogy of the xenoliths, dominated by fassaite diopside, suggests further contact thermal metamorphism of the xenoliths as the LHZBG magmas continued to flow through the conduit. This would have resulted in modification (coalescence) of the pyrite grains, giving the blebby texture observed in the xenoliths.

The xenoliths' precursor minerals, such as fassaite diopside, may have suffered retrograde metamorphism as any water remaining in the xenolith was driven off by the intrusion of the LHZBG magma. The finger structures of LHZBG Unit material in the xenoliths suggest that the LHZBG magma may have been able to intrude the xenoliths, possibly allowing the introduction of late stage fluids into the xenoliths. The chlorite occurrence in the xenoliths may reflect this.